

HAWKING RADIATION FROM NON-EVAPORATING PRIMORDIAL BLACK HOLES CANNOT ENABLE THE FORMATION OF DIRECT COLLAPSE BLACK HOLES

JONATHAN REGAN^{1,2,*} , MARIOS KALOMENOPOULOS² , AND KELLY KOSMO O'NEIL¹ ¹ Department of Physics, University of Nevada, Reno² Department of Physics and Astronomy, University of Nevada, Las Vegas*Version March 18, 2025*

ABSTRACT

The formation of supermassive black holes (SMBHs) in the early Universe is a subject of significant debate. In this study, we examine whether non-evaporating primordial black holes (PBHs) can offer a solution. We establish initial constraints on the range of PBH masses that correspond to Hawking radiation (HR) effective temperatures in the range needed to suppress H_2 cooling, which would facilitate the formation of massive black hole seeds in atomic cooling halos. We also investigate the specific intensity of the HR from non-evaporating PBHs and compare it with the critical radiation needed for direct collapse black holes (DCBHs). We show that HR from non-evaporating PBHs cannot serve as an irradiating mechanism to facilitate the formation of the seeds for the SMBHs we observe in the high-redshift Universe unless, perhaps, the PBHs within the relevant mass range comprise a significant fraction of dark matter and are significantly clustered towards the center of the primordial halo.

Subject headings: Hawking Radiation, Primordial Black Holes, Supermassive Black Holes

1. INTRODUCTION

In the standard model of cosmology, our Universe is expanding from a hot and dense state (e.g. Workman et al. 2022). Astrophysical structures begin to form when initial fluctuations collapse to form the first gas clouds (also known as primordial gas clouds). These are the birthplaces of the first galaxies (e.g. Johnson et al. 2012; Yajima et al. 2017; Cimatti et al. 2020; Volonteri et al. 2021). Many, if not all, of these galaxies are believed to harbor a massive black hole (BH) in their center. Observations of quasars formed in the early Universe indicate that a number of these BHs have masses of more than a billion solar masses, and were formed before the Universe was a billion years old¹. The formation of these high-mass black holes, aptly called supermassive black holes (SMBHs), is a matter of considerable debate (e.g. Rees 1984; Inayoshi et al. 2020).

Three of the most prevalent proposed scenarios, outlined in Rees (1984), include: 1) the collapse of massive Pop III stars and their growth due to accretion (Omukai 2001; Yajima & Khochfar 2016; Klessen 2019; Latif et al. 2022b), 2) runaway mergers in dense star clusters (Katz 2019), and 3) the ‘direct collapse’ scenario. There are many mechanisms proposed for the latter, including the abrupt collapse of a metal-free (or metal-poor) gas cloud due to the suppressing role of Lyman-Werner (LW) radiation on molecular cooling due to H_2 , dynamical heating, streaming motions of baryon-dark matter, the increase of the mass of protostellar collapse in the presence of magnetic fields, or gas dynamical processes (Begelman et al. 2006; Lodato & Natarajan 2006; Schleicher et al. 2009; Begelman 2010; Shang et al. 2010; Agarwal et al. 2012, 2014; Hirano et al. 2017; Agarwal 2019; Latif 2019; Latif et al. 2021; Hirano et al. 2021; Latif et al. 2022a, 2023; Regan & Volonteri 2024; Chon & Omukai 2024). Alternative scenarios, among others, involve the growth of primordial black holes (PBHs) (Bean & Magueijo 2002; Dückting 2004). For a more detailed coverage of these and other scenarios, see (Volonteri 2010; Latif & Ferrara 2016; Becerra 2018; Smith & Bromm 2019; Inayoshi et al. 2020; Haemmerlé et al. 2020; Volonteri et al. 2021).

Even the most common proposals are not without problems. For example, a newly-born Pop III star in the range of $\sim 100 M_\odot$ would need to accrete continuously at a rate close to the Eddington limit for at least a Gyr to reach masses close to $10^9 M_\odot$ at redshifts $z = 6 - 7$ (Milosavljević et al. 2009; Latif & Ferrara 2016; Smith & Bromm 2019), which poses difficulties for the first scenario. Dense star clusters would need to be able to retain their members after the mergers (i.e. to overpower the gravitational kicks that lead to the ejection of the merged object from the cluster (Merritt et al. 2004; Loeb & Furlanetto 2013)), posing difficulties for the second scenario.

*E-mail: jonathan.regan@unlv.edu, jonathanregan12@gmail.com

¹ Such as the quasar ULAS J1342+0928, whose SMBH has a mass of 800 million solar masses (Bañados et al. 2017). See also (Wu et al. 2015; Mortlock et al. 2011; Fan et al. 2003; Inayoshi et al. 2020).

This paper focuses on the third scenario: the direct collapse of metal-poor gas clouds, a ‘heavy seeds’ scenario. In this case, the masses of the initial BHs can reach up to $10^5 - 10^6 M_\odot$ (e.g. Agarwal et al. 2014; Woods et al. 2017) due to general relativistic instabilities². Therefore, they could grow through more viable rates of accretion into the SMBHs we observe by $z \approx 6 - 7$. One of the usual prerequisites for this scenario is to avoid fragmentation of the initial gas cloud to many smaller stars, and instead form directly a single, supermassive star that would lead to a massive BH³. In reality, the situation is more complex, and it is still uncertain whether fragmentation can be completely avoided or if it is a basic prerequisite for heavy seed formation (Klessen & Glover 2023; Liu et al. 2024). Studies have shown that it is still possible to form a massive BH seed, even in the presence of moderate fragmentation. The key in these cases is high accretion rates (i.e. $\dot{M} > 0.1 M_\odot/\text{year}$) of the protostars so that they can grow rapidly with negligible radiative feedback and an enhanced cross-section for collisions, which would allow the merging of numerous fragments (Omukai & Palla 2001; Reinoso et al. 2023; Boekholt et al. 2018) (for some alternative direct-collapse scenarios see also e.g. (Mayer & Bonoli 2019; Latif et al. 2022a)). In all cases, it is highly preferential that the collapse of the gas be delayed to happen in an ‘atomic cooling cloud’ - a cloud without significant metals or molecules that could cool efficiently - so that high accretion rates can be achieved. Such a cloud could form if production of H_2 , the main coolant in the early Universe, is suppressed. This can be accomplished by a number of mechanisms (Inayoshi et al. 2020; Regan et al. 2020; Wise et al. 2019; Visbal et al. 2014b). In this paper, we consider the presence of strong UV radiation in the LW range (11.2 – 13.6 eV) that is able to suppress the formation of molecular hydrogen H_2 (Omukai 2001; Oh & Haiman 2002; Bromm & Loeb 2003; Agarwal & Khochfar 2015; Agarwal et al. 2019) through radiation from PBHs.

For this mechanism, we investigate whether the Hawking radiation (HR) (Hawking 1974) emitted from early-Universe PBHs (Hawking 1971; Carr & Hawking 1974) can create the necessary conditions for the formation of large BH seeds via the direct collapse of primordial gas clouds. In this proposed mechanism, the required photons are supplied by the HR of an evaporating PBH that is still far from “exploding”. We model this radiation as a blackbody spectrum, focusing only on primary photon emission.

The role of PBHs in the formation of the first stars and galaxies has been investigated before (Liu et al. 2022; Liu & Bromm 2023; Lu et al. 2024), but remains an important unanswered question in the scientific community. Most recently, Lu et al. (2024) studied the heating effects of secondary HR spectra from “exploding” PBHs in primordial gas clouds. They find that in the presence of significant clustering of the PBHs in the clouds, PBHs of masses on the order of 10^{14} g can lead to a successful direct collapse of the cloud. On the other hand, Liu et al. (2022); Liu & Bromm (2023) used cosmological simulations and semi-analytical models to explore the effects of stellar-mass ($\sim 10 - 100 M_\odot$) PBHs in the acceleration of structure formation and gas heating by accretion feedback on the BHs. In the former case, they find that structures are similar to the ones found in Λ CDM simulations, but in latter case, they show that LW photons from accretion onto stellar-mass PBHs in the halo can indeed promote the formation of massive seeds through the direct-collapse scenario. In this work, we describe a simplified and easily-modifiable analysis framework, more in line with Lu et al. (2024), in hopes that the scientific community can continue to build on this work to answer this open question.

For all cosmological calculations in this paper, we assume a flat Λ CDM cosmology with $H_0 = 70 \text{ km/s/Mpc}$ and $\Omega_m = 0.3$. This paper is organized as follows: Section 2 reviews the main consequences of Hawking radiation. Section 3 introduces some of the relevant features of primordial black holes. Section 4 sets constraints on the primordial black holes that could act as sources of the Hawking radiation needed to produce ‘heavy seeds’, and compares these constraints with current observational limits. Finally, Section 5 provides a comprehensive discussion of the assumptions and caveats of this work and proposes extensions to this simplified model.

2. HAWKING RADIATION

This section provides a review of the main consequences of HR from a BH. We assume a Schwarzschild BH, ignoring spins which are expected to be very small in most cases for PBHs (De Luca et al. 2019; Mirbabayi et al. 2020) that we consider in Section 3, and consider only its primary photon emission. For a discussion on the validity of these assumptions, see Section 5.

2.1. Blackbody spectrum

The main component of HR can be modeled as a blackbody spectrum,

$$B_\nu = f_\Gamma f_{\text{ph}} \frac{2h\nu^3}{c^2} \frac{1}{\exp[h\nu/k_B T] - 1}, \quad (1)$$

where all the constants and variables have their usual meaning⁴ and f_{ph} refers to the percentage of HR that is in

² We note though that recent simulation results (Regan & Volonteri 2024; Liu et al. 2024) show that there is not a clear-cut, bimodal distribution between ‘heavy’ and ‘light’ seeds, and there are mechanisms that produce heavy BHs as the tails of a continuum mass spectrum.

³ The presence of angular momentum is also an obstacle to massive BH collapse that needs to be overcome. Here, we assume that the gas clouds in question have overcome this issue by assuming they have either formed with negligible angular momentum, or that they have lost their initial angular momentum due to interactions with their environment (Koushiappas et al. 2004) and/or primordial magnetic seed fields (Hirano et al. 2021)

⁴ More specifically: ν is the frequency of emitted photons, T is the temperature of the blackbody, h is Planck’s constant, c is the speed of light, and k_B is Boltzmann’s constant.

photons, with $f_{\text{ph}} = 1$ denoting the case where all of the HR is in photons. We use $f_{\text{ph}} = 0.2$ (Page 1976), unless stated otherwise. f_{Γ} corresponds to a constant ‘greybody’ factor of $f_{\Gamma} = 0.24$, as described in Section 5.2.

According to Hawking’s analysis (Hawking 1974), the temperature of a BH is connected to its mass via the expression

$$T_{\text{BH}} = \frac{\hbar c^3}{8\pi k_B G M_{\text{BH}}} \simeq 6.17 \times 10^{-8} \left(\frac{M_{\odot}}{M_{\text{BH}}} \right) \text{ K}, \quad (2)$$

where M_{BH} is the mass of the black hole and G is Newton’s gravitational constant. Hence, the temperature of a BH is inversely proportional to its mass. This is a feature we will exploit in Section 4.

Eqs. (1) and (2) can then be combined to get the blackbody spectrum as a function of mass:

$$B_{\nu} = f_{\Gamma} f_{\text{ph}} \frac{2h\nu^3}{c^2} \frac{1}{\exp[16\pi^2 G M_{\text{BH}} \nu / c^3] - 1}. \quad (3)$$

2.2. Mass evolution and evaporation time

The energy of the emitted radiation comes from the BH, which in turn “loses” its mass. As a result, the temperature of the blackbody increases, as does the peak energy of radiation, leading to increased mass loss. Equating the energy emitted to the Stefan-Boltzmann luminosity provides the evolution of the BH mass with time:

$$-\frac{dM_{\text{BH}}}{dt} c^2 = L \Rightarrow \frac{dM_{\text{BH}}}{dt} c^2 = -A\sigma T^4 = -16\pi \left(\frac{GM_{\text{BH}}}{c^2} \right)^2 \left(\frac{\hbar c^3}{8\pi G M_{\text{BH}} k_B} \right)^4, \quad (4)$$

where A is the Schwarzschild surface area and σ is the Stefan-Boltzmann constant.

Solving eq. (4), assuming $t_{\text{initial}} \rightarrow 0$, the time evolution of the BH mass since the Big Bang is:

$$M_{\text{BH}}(t) = \left[M_i^3 - \frac{3}{256} \frac{c^6 \sigma}{\pi^3 G^2} \left(\frac{\hbar}{k_B} \right)^4 t \right]^{1/3} = [M_i^3 - C \cdot t(z, H_0, \Omega_m)]^{1/3}, \quad (5)$$

with

$$C = 4.76 \times 10^{-59} M_{\odot}^3 / \text{Gyr}.$$

The very small value of this constant indicates that there are no significant changes in mass until the very final moments of BH evaporation.

The evaporation time t_{ev} of a BH is the amount of time required for it to completely evaporate due to the emission of HR. Setting $M_{\text{BH}}(t_{\text{ev}}) = 0$ in eq. 5, it is straightforward to find:

$$t_{\text{ev}} = \frac{15360\pi G^2 M_{\text{BH}}^3}{3\hbar c^4} = 2.1 \times 10^{67} \left(\frac{M_{\text{BH}}}{M_{\odot}} \right)^3 \text{ yr}. \quad (6)$$

As such, the maximum mass of a BH that could have evaporated due to HR within the age of the Universe (~ 13.7 Gyr) is $\sim 9 \times 10^{-20} M_{\odot}$ (or $\sim 1.8 \times 10^{14}$ g). If one takes into account the larger variety of particles emitted as a BH evaporates (other than photons), then the evaporation time becomes shorter (Mosbech & Picker 2022). We comment more on this in Section 5.

Finally, the time evolution of HR temperature is given by inserting the mass evolution, eq. (5), into the HR temperature, eq. (2):

$$T = \frac{\hbar c^3}{8\pi k_B G} \frac{1}{[M_i^3 - C \cdot t(z, H_0, \Omega_m)]^{1/3}}. \quad (7)$$

For the BHs of interest in this work, the temperatures remain effectively constant over relevant timescales, as confirmed in Figure (5). As such, we ignore the effects of time evolution in the analysis from this point on.

3. PRIMORDIAL BLACK HOLES

This work investigates whether HR from PBHs can act as an irradiation source of primordial gas clouds, facilitating their collapse into DCBHs. Since the latter demands temperatures of the order of 10^4 K, this requires BHs with masses

much smaller than $1 M_{\odot}$ (see Section 4). A natural candidate for the source of HR in this scenario is primordial black holes.

PBHs are standard black holes formed in the early stages of the Universe when density fluctuations surpass a specific threshold (e.g. Hawking 1971; Carr & Hawking 1974; Carr 1975; Carr & Kühnel 2020). PBHs are well known as possible dark matter candidates, and most importantly ones that do not require any "new physics" to explain. The birth, lifespan, and ultimate collapse of a PBH are all based on concepts of general relativity. PBHs may also contribute to a number of other phenomena including lensing, gravitational wave events, and growth of structure in the high-redshift Universe (e.g. Escrivà et al. 2022).

The (maximal) mass of a PBH at formation time, assuming a period of a radiation-dominated universe, is comparable to the horizon mass (Byrnes & Cole 2021; Arbey 2024):

$$M_{\text{PBH}} \sim M_H = \frac{4}{3} \pi \rho \left(\frac{1}{H} \right)^3 \sim 10^{15} \left(\frac{t}{10^{-23} \text{ s}} \right) \text{ g}, \quad (8)$$

where t is the time since the Big Bang. The reference mass of 10^{15} g corresponds to a PBH that will be evaporating today due to HR. In contrast, at $t \sim 1$ s (redshift $z \sim 10^9$ based on Λ CDM), the mass of a PBH can be on the order of $\sim 10^5 M_{\odot}$. As such, the range of possible PBH masses spans many orders of magnitudes.

PBHs have not yet been observed, but a number of constraints have been placed on them through indirect methods either via their gravitational effects or due to their radiation effects from HR and accretion (e.g. Rice & Zhang 2017; Carr et al. 2021; Green & Kavanagh 2021; Auffinger 2023). These constraints are generally phrased in terms of the fraction of dark matter (DM) occupied by PBHs, $f_{\text{PBH}} = \rho_{\text{PBH}} / \rho_{\text{DM}}$, where $f_{\text{PBH}} = 1$ would correspond to the PBHs making up all of the DM. The filled regions of Figure 1 show some of the main observational constraints from Green & Kavanagh (2021). Excluding the range of masses where f_{PBH} remains effectively unconstrained ($\sim 10^{17} - 10^{21}$ g or $10^{-17} - 10^{-12} M_{\odot}$, as well as the most massive PBHs), $f_{\text{PBH}} < 0.1$ in all of the other mass ranges. Note that the constraints are model dependent, and the numbers quoted above are optimistic limits (for some ranges, $f_{\text{PBH}} \ll 1$).

4. HR FROM PBHS AS A SOURCE OF DCBHS

The key criteria required for the formation of DCBHs in the scenario considered here include:

- The presence of radiation that would be able to dissociate or suppress the formation of molecular H_2 , the main coolant in the early Universe (Agarwal 2019). This can be achieved with strong UV radiation in the LW range (11.2 – 13.6 eV) directly, and indirectly with the destruction of H^- , a dominant intermediate species in the formation of H_2 , by irradiation of photons with energy $E_{\gamma} \gtrsim 0.8$ eV (Sugimura et al. 2014). We discuss both cases below (Sections 4.2 and 4.3), together with the contribution of other radiation feedback. Our main emphasis is in the LW band.
- The presence of radiation with a strength of $J_{\text{crit}} \sim 10 - 10^5$ in conventional units of $10^{-21} \text{ erg/s/cm}^2 / \text{Hz/sr}$. In practice, we do not use a universal J_{crit} , but a critical value that depends on the radiation temperature, following the prescription in Sugimura et al. (2014). For more details, see Section 4.4.
- The above contribute to the delayed collapse of a gas cloud at redshifts in the range $[z \in (10, 30)]$, inside a massive atomic cooling halo, where significant accretion rates are possible. Then, the formation of a massive BH seed is likely.

In this section, we investigate whether we can satisfy the above criteria with the presence of PBHs. In other words, in the redshift range of interest $[z \in (10, 30)]$, is it feasible for a population of PBHs to emit blackbody radiation with effective temperature T_{crit} and with enough intensity in the frequency ranges of interest to surpass J_{crit} ?

4.1. Constraints from evaporation redshift

The scenario investigated in this work requires that the PBHs have not evaporated before $z_{\text{min}} = 10$. This sets a lower limit to the masses of PBHs of interest, i.e. $M_{\text{PBH}} > M_{\text{evap}}$. Assuming the fiducial cosmological model, $z = 10$ corresponds to an age of the universe $t_{\text{age}}(z = 10) = t_{\text{age},10} \sim 0.47$ Gyr. Equating this with evaporation time, and demanding $t_{\text{evap}} \gtrsim t_{\text{age},10}$, we get a mass constraint: $M_{\text{evap}} \gtrsim 2.8 \times 10^{-20} M_{\odot}$ (or 5.5×10^{13} g).

4.2. Constraints from X-ray feedback

The effect of X-rays in the chemistry of the gas cloud is complicated, especially when it is present simultaneously with a LW background (Ricotti 2016; Park et al. 2021). On the one hand, they can provide positive radiative feedback to star formation by enhancing production of H_2 , and hence cooling. On the other, an intense X-ray background can provide heating that prevents gas collapse (Haiman et al. 2000; Park et al. 2021).

As a first step to estimate these effects, we find the PBH masses where LW photons are stronger than X-ray photons by calculating the ratio $B_{\text{LW}}(M_{\text{BH}})/B_{\text{X-rays}}(M_{\text{BH}}) \gtrsim 1000$. B_{LW} denotes the (blackbody) specific intensity at the center of the LW band (12.5 eV), and $B_{\text{X-rays}}$ denotes the specific intensity of X-ray photons at an energy of 1 keV and 0.2 keV. This leads to a mass constraint: $M_{\text{x-ray},1\text{keV}} \gtrsim 1.0 \times 10^{-13} M_{\odot}$ (or 2.0×10^{20} g) and $M_{\text{x-ray},0.2\text{keV}} \gtrsim 4.0 \times 10^{-13} M_{\odot}$ (or 8.0×10^{20} g). This constraint poses a more stringent lower limit than the evaporation constraint described above.

For our constraints, we used estimates for the ratio of specific intensities and energies (which in our case are equivalent since we consider the PBHs as the sources of both) from Figure 3 of Ricotti (2016) and Figure 5 of Park et al. (2021). Both papers study situations of realistic minihalos in a joint LW and X-ray background, and generally find that the presence of strong X-ray radiation can lead to faster fragmentation and production of multiple Pop III stars in lower-mass halos. Note that the ratios they report correspond to a LW background of significant intensity, i.e. $J_{\text{LW},21} > 10^{-2}$, which is much bigger than what we find below. Nevertheless, in our case we use their estimates simply as a guide to the masses of interest, similar to Section 4.1.

4.3. Constraints from critical temperature

This scenario also requires that the PBHs emit a blackbody spectrum above the threshold temperature to suppress H_2 formation and delay gas collapse to a massive atomic cooling halo ($T_{\text{crit}} \sim 8000$ K) (Sugimura et al. 2014). This temperature corresponds to photons of energy $E_{\nu} = 2.0$ eV, which are required for the photodissociation of H^- , an important element in the process of H_2 production. This sets an upper limit to the masses of PBHs of interest, i.e. $M_{\text{PBH}} < M_{\text{crit}}$. From eq. (2), we get a mass constraint: $M_{\text{crit}} \lesssim 7.5 \times 10^{-12} M_{\odot}$ (or 1.5×10^{22} g).

The constraints reported in Sections 4.1, 4.2 and 4.3 are necessary but not sufficient conditions for PBHs to act as the appropriate radiation sources to decrease the cooling rates of the primordial gas clouds. These constraints simply establish the range of masses that are relevant for this scenario, which is graphically depicted by the dashed lines in Figure 1. Note that these mass limits do not pose any restrictions to f_{PBH} ; they simply point to the PBH masses that are required for this mechanism to be valid. Interestingly, the T_{crit} and X-ray constraints demand masses in a region of f_{PBH} parameter space that remains predominantly open: $4.0 \times 10^{-13} M_{\odot} \lesssim M_{\text{PBH}} \lesssim 7.5 \times 10^{-12} M_{\odot}$.

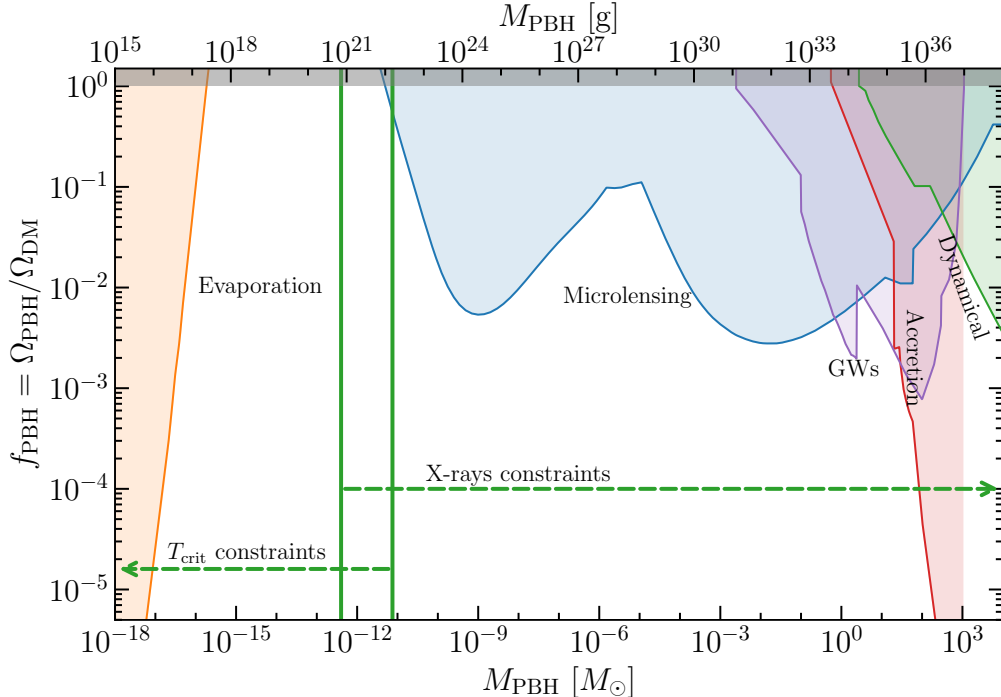


FIG. 1.— Constraints on the fraction of DM in PBHs from different methods (filled regions - Hawking evaporation (orange), gravitational lensing constraints on compact objects (blue), constraints from a stochastic background and individual gravitational wave mergers (purple), accretion on PBHs (red), dynamical constraints on compact objects (green)), based on Green & Kavanagh (2021) and plotted using PBHbounds^a. The dashed lines show mass ranges that satisfy the respective constraints labeled above the arrows. These are physical constraints on the masses of PBHs that are needed to satisfy some of the DCBH formation criteria, as described in Sections 4.2 and 4.3. The constraints based on evaporation redshift, i.e. that the PBHs have not evaporated by $z = 10$ - see Section 4.1, are not plotted here since the allowed region from that constraint spans the full plot. The y-axis values on the constraints are arbitrary and chosen for clearer visualization.

^aWhich can be found [here], with the official release [here]. The filled contour constraints are made from a combination of multiple individual constraints that belong to each category. For detailed references, we refer to Green & Kavanagh (2021).

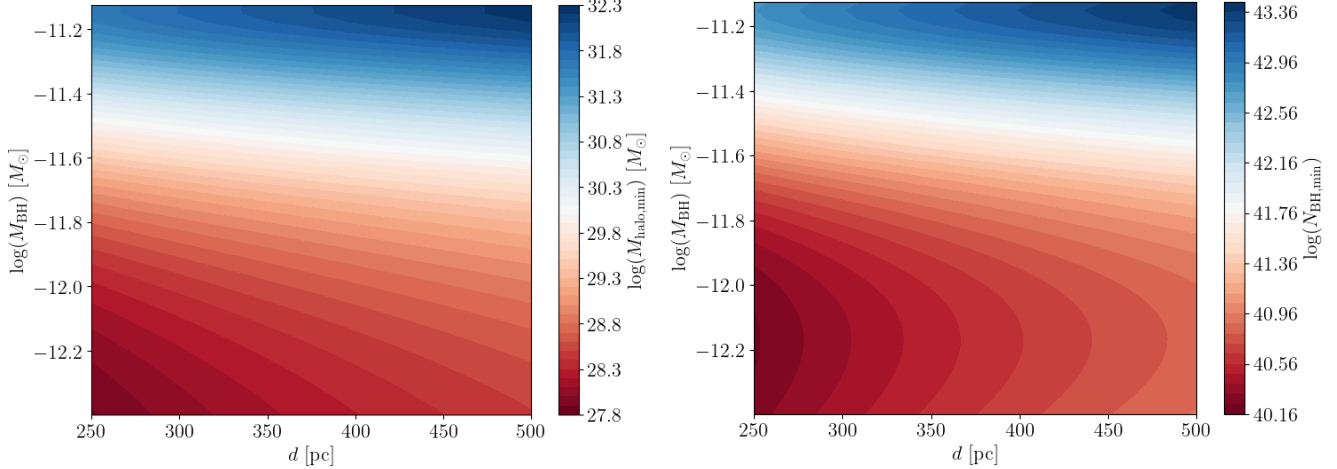


FIG. 2.— (a) Minimum estimated PBH halo mass (as a function of PBH mass and distance) that is required to produce $J_{21,\text{LW}}^{\text{tot}} \gtrsim J_{\text{crit}}(M_{\text{PBH}})$ for the simplest scenario considered in this work: a population of monochromatic PBHs within the mass range of interest at a distance d from a primordial gas cloud. The minimum mass of the PBH halos that satisfy this condition ($M_h \sim 10^{27.8} M_\odot$) are many orders of magnitudes larger than the most massive DM halos expected, rendering this scenario unphysical. (b) Same as (a), but parameterized in terms of the minimum number of PBHs that are required in order to reach $J_{21,\text{LW}}^{\text{tot}} \gtrsim J_{\text{crit}}(M_{\text{PBH}})$. For the distances, we adopt the range [250, 500] pc, to compare with Visbal et al. (2014b). This range ensures the halos to not be tidally disrupted by their interactions, but be close enough for the LW intensity from stars to be significant. See section 4.4.1 for more details.

4.4. Constraints from critical radiation intensity

In this section, we investigate whether it is feasible for PBHs within the mass range of interest (determined in Sections 4.1, 4.2 and 4.3) to provide the critical radiation intensity (CRI) J_{crit} needed to prevent the collapse of the initial cloud, in order to happen in a massive, atomic-cooling halo to achieve high accretion rates. CRI is given in units of $\text{erg/s/cm}^2/\text{Hz/sr}$, and is commonly normalized with respect to $J_{21} = 10^{-21} \text{ erg/s/cm}^2/\text{Hz/sr}$ (Bromm & Loeb 2003; Loeb & Furlanetto 2013; Sugimura et al. 2014).

Across the literature, there are a number of different estimates for the CRI needed to keep the primordial cloud heated (e.g. Agarwal & Khochfar 2015; Agarwal et al. 2016a; Agarwal et al. 2016b, 2017; Latif & Khochfar 2019; Agarwal et al. 2019). These estimates depend on several key features such as the relevant radiation source and its spectrum, the spatial configuration of the halo, and the cosmological setting, with J_{crit} ranging from ~ 1 to 10^5 (e.g. Omukai 2001; Bromm & Loeb 2003; Shang et al. 2010; Visbal et al. 2014b; Agarwal & Khochfar 2015; Agarwal et al. 2016a; Latif & Ferrara 2016; Wolcott-Green et al. 2017; Incattasciato et al. 2023). In our approach, we follow Sugimura et al. (2014), and adopt a J_{crit} that depends on the radiation temperature. More specifically, Sugimura et al. (2014) provides a fitting formula for J_{crit} with respect to the ratio of photodissociation coefficients of H^- , H_2 , i.e. $J_{\text{crit}} = f(k_{H^-}/k_{H_2})$, which in turn depends on the temperature of the blackbody spectrum. In our case, we connect the temperature of the HR to the masses of the PBHs, and have a mass-depended critical intensity $J_{\text{crit}} = f(M_{\text{PBH}})$. We note that their fitting formula is valid for a temperature range $T \in (8000, 2 \cdot 10^5)$ K, which is consistent with our temperature constraints in Section 4.3. For our range of masses, the minimum and maximum J_{crit} are 5.12 and 1400 respectively in the standard J_{21} units.

We note that recent studies (Schauer et al. 2021; Kulkarni et al. 2021; Muñoz et al. 2022) also show that the presence of streaming velocities generally compliments the effects of LW radiation, allowing heavy seed formation even under moderate fragmentation. The relative importance of the two mechanisms - streaming velocities and LW radiation intensity - depends on redshift, with the former dominating at early times and the latter dominating at redshifts $z \lesssim 15$. Although these works analyze the critical (minimum) mass of dark matter halos required for PopIII star formation, compared to the status of gas clouds investigated in our case, the CRI found is only approximately one order of magnitude smaller than the values we consider, so it does not change the conclusions presented here.

To provide an easily-reproducible analysis framework for the scientific community, we follow Liu et al. (2022); Liu & Bromm (2023) by treating the LW radiation from the PBHs as a ‘background’ and ignoring self-shielding – the idea that a fraction of the outer layer of the gas protects the inner layer from radiation, allowing it to cool.

A BH with Schwarzschild radius R_S emits HR with luminosity $L_{\text{LW}} = 4\pi^2 R_S^2 B_{\text{LW}}$. Its flux at distance d and solid angle $\Omega = 4\pi \text{ sr}$, assuming spherical geometry, give a specific intensity:

$$J_{\text{LW}} = \frac{B_{\text{LW}}}{4} \left(\frac{R_S}{d} \right)^2. \quad (9)$$

In standard units, this becomes:

$$J_{21,\text{LW}} = 10^{21} \frac{B_{\text{LW}}}{4} \left(\frac{R_S}{d} \right)^2. \quad (10)$$

In the following subsections, we investigate several different PBH spatial distributions. Unless stated otherwise, we calculate PBH densities assuming the most optimistic limit of $f_{\text{PBH}} = 1$, which is allowed for the mass range found in Sections 4.1, 4.2 and 4.3. Note that we do not present results for different mass distributions because we show in Appendix 9.3 that a population of monochromatic PBHs is sufficient to test the viability of the scenario at hand.

4.4.1. Constant distance & monochromatic PBHs

The simplest case, as explored in Visbal et al. (2014b); Wise et al. (2019), is a cluster of monochromatic PBHs at a distance d from a primordial gas cloud that irradiates the cloud with LW HR photons⁵. For N_{BH} black holes of the same mass, the total intensity is $J_{21,\text{LW}}^{\text{tot}} = N_{\text{BH}} \cdot J_{21,\text{LW}}$. We find N_{BH} , by demanding that $J_{21,\text{LW}}^{\text{tot}} > J_{\text{crit}}(M_{\text{PBH}})$. Figure 2(a) shows an approximation of the total PBH halo mass ($M_{\text{PBH,halo}} = N_{\text{BH}} M_{\text{BH}}$) as a function of distance d for the range of allowed PBH masses. Even for the most optimistic combinations of d and M_{BH} , the total halo mass required for this scenario ($M_{\text{h}} \sim 10^{27.8} M_{\odot}$) exceeds the expected halo mass function at $z > 10$ by several orders of magnitude (e.g. Lovell et al. 2023; O’Brennan et al. 2024), indicating that such a configuration is not valid for the PBHs of interest here. Of course, this remains the case even if the lower limit of $J_{21,\text{LW}}$ is used. Figure 2(b) shows the actual number of PBHs required for a specific combination of mass and distance.

Note that here we do not consider the DCBH-formation timescale. In contrast, Visbal et al. (2014b) considers a timescale of $t_{\text{coll}} \sim 10$ Myr. Both approaches are valid given the different mechanisms in the two situations. In (Visbal et al. 2014b), they consider that the LW radiation is provided by the second member of a pair of atomic cooling halos, which manages to form stars first. The latter are the source of the LW photodissociating radiation and evolve in similar timescales as the collapse. In our case, as shown in Appendix 9.2, the time evolution of PBHs is negligible for the redshift and mass ranges of interest. In other words, emission is expected to be constant for the whole period of collapse by default.

4.4.2. Uniform distribution & monochromatic PBHs

Next, we consider a population of monochromatic PBHs that are uniformly distributed inside the halo from a minimum radius r_{min} to a maximum radius r_{max} . This maximum radius is based on an estimate of the halo size, as explained in Appendix 9.1. The choice of minimum value is arbitrary, but motivated from Liu et al. (2022), who find that stellar-mass PBHs can reach distances on the order of ~ 1 pc from the center of the DM halo. We choose $r_{\text{min}} = 1$ pc, unless stated otherwise, to be able to compare between the two scenarios.

The density of a uniform-density shell of volume $V_{\text{shell}} = 4\pi(r_{\text{max}}^3 - r_{\text{min}}^3)/3$ is given by:

$$\rho = \rho_{\text{vir}} = \rho_0 = \frac{M_{\text{tot}}}{V_{\text{shell}}} = \frac{N_{\text{BH}} M_{\text{BH}}}{V_{\text{shell}}}. \quad (11)$$

The number of PBHs within the shell is then given by:

$$N_{\text{BH}} = \frac{\rho_0}{M_{\text{BH}}} \cdot \frac{4}{3}\pi(r_{\text{max}}^3 - r_{\text{min}}^3), \quad (12)$$

or for a thin shell, the differential number of PBHs is:

$$dN_{\text{BH}} = \frac{\rho_0}{M_{\text{BH}}} \cdot 4\pi r^2 dr. \quad (13)$$

Then for the whole volume, the total LW radiation intensity at the center of the halo is:

$$J_{21,\text{LW}}^{\text{tot}} = \int_{r_{\text{min}}}^{r_{\text{max}}} dN_{\text{BH}} J_{21,\text{LW}} = 10^{21} \frac{\pi B_{\text{LW}} R_S^2 \rho_0}{M_{\text{BH}}} (r_{\text{max}} - r_{\text{min}}) = 10^{21} \frac{\pi B_{\text{LW}} R_S^2 \rho_0 r_{\text{min}}}{M_{\text{BH}}} \left(\frac{r_{\text{max}}}{r_{\text{min}}} - 1 \right). \quad (14)$$

The blue line in the top left panel of Figure 3 shows the specific intensity of LW photons at the center of a halo as a function of total halo mass. Even for the largest halo masses in this case, the radiation intensity is many orders of magnitude lower than the CRI needed to form a DCBH. Note that varying the minimum radius, redshift, and PBH mass affects the total radiation intensity slightly – as explored in the following subsection for the isothermal case – but not enough to reach the required J_{crit} . As with the case of monochromatic PBHs at a constant distance, a uniform distribution of monochromatic, non-evaporating PBHs similarly cannot enable the collapse of a DCBH.

⁵ For simplicity, we focus on photons in the middle of the energy range, i.e. we take $E_{\gamma} = 12.5$ eV. Alternatively, one can integrate $\int_{\nu_1}^{\nu_2} L_{\nu} d\nu$ and divide by $\Delta\nu$.

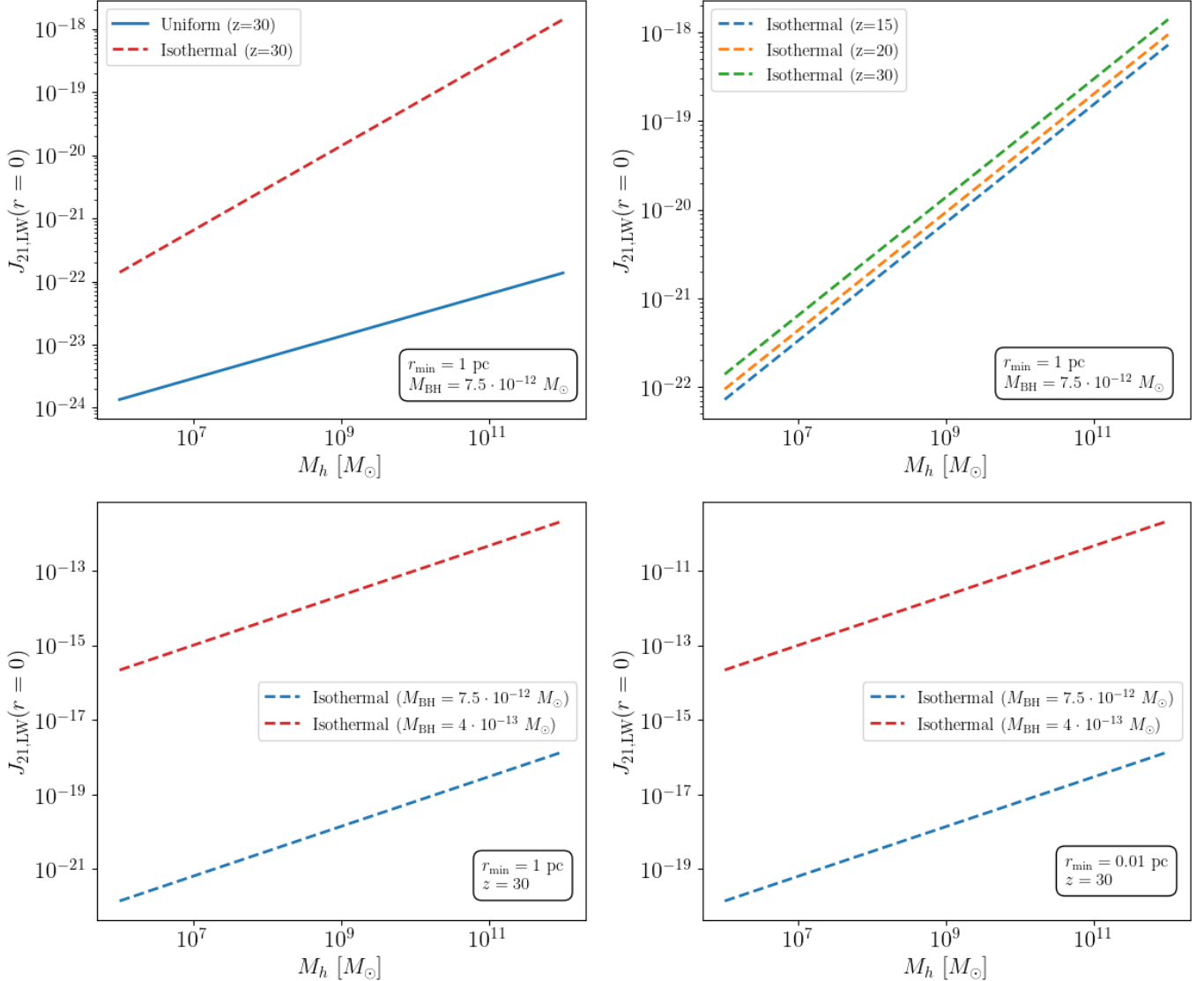


FIG. 3.— Specific intensity at the center of the halo for different halo masses. PBHs are distributed within the halo based on a uniform or isothermal density (Section 4.4.2 versus Section 4.4.3). The four panels of this figure investigate the effects of different density profiles (top left), of different initial redshifts of collapse (top right), of different PBH masses (bottom left), and of different minimum distances that the PBHs can reach inside the halo (bottom right). The density at r_{\max} is set to the virial density $\rho_0 = \rho_{\text{vir}}$, as described in Appendix 9.1. The emitted specific intensity for all cases that we investigate remains orders of magnitude below the CRI required for collapse ($5.12 \lesssim J_{\text{crit}} \lesssim 1400$), indicating that HR from non-evaporating PBHs is not in itself a sufficient mechanism for the formation of DCBHs in the early Universe.

4.4.3. Isothermal distribution & monochromatic PBHs

For a more realistic case, we investigate a monochromatic population of PBHs that follow an isothermal distribution (e.g. Wise et al. 2019; Liu et al. 2022). Here, the density scales as $\rho = \rho_0(r_{\max}/r)^2$, where the density equals the virial density of the halo for $r = r_{\max}$.

In this case, the total LW radiation intensity from the shell at the center of the halo is:

$$J_{21,\text{LW}}^{\text{tot}} = \int_{r_{\min}}^{r_{\max}} dN_{\text{BH}} J_{21,\text{LW}} = 10^{21} \frac{\pi B_{\text{LW}} R_{\text{S}}^2 \rho_0 r_{\max}^2}{M_{\text{BH}}} \int_{r_{\min}}^{r_{\max}} \frac{dr}{r^2} = 10^{21} \frac{\pi B_{\text{LW}} R_{\text{S}}^2 \rho_0 r_{\max}}{M_{\text{BH}}} \left(\frac{r_{\max}}{r_{\min}} - 1 \right). \quad (15)$$

Comparing this case with eq. (14) gives:

$$J_{21}^{\text{isothermal}} = (r_{\max}/r_{\min}) J_{21}^{\text{uniform}}. \quad (16)$$

Since $r_{\max} > r_{\min}$ and thus $J_{21}^{\text{isothermal}} > J_{21}^{\text{uniform}}$, an isothermal distribution of PBHs will provide a specific intensity of LW photons that is closer to the required J_{crit} value than a uniform distribution of PBHs will, as demonstrated in the top left panel of Figure 3. However, even for the largest halos, the specific intensity still falls several orders of

magnitude short of the required J_{crit} for this scenario.

Figure 3 also shows the effects of varying other parameters such as the minimum distance of the PBHs from the center, the formation redshift, and the PBH masses within the allowed ranges. None of these cases provide a radiation intensity that reaches the required J_{crit} value, even in the more optimistic scenario where $J_{\text{crit}} \sim 5$. We find that to reach $J_{\text{crit}} \sim 5$, in redshift $z \sim 30$ for a halo of mass $M_h \sim 10^{-13} M_\odot$ – the more optimistic scenario – would require an $r_{\text{min}} \sim 3$ km. This is unphysical, if one considers that the Schwarzschild radius of a BH with $M_{\text{BH}} \sim 10^5 M_\odot$ (which would be the approximate mass of the seed BH at the center) would be much bigger than that.

Hence, the investigated radiation mechanism provides a LW intensity many orders of magnitude smaller than critical, yielding it an ineffective way of creating the seeds of massive BHs in the early Universe.

4.4.4. LW background from monochromatic PBHs

Finally, we consider the effects of the PBHs' LW radiation acting as a cosmological background (Haiman et al. 1997; Visbal et al. 2014a). To calculate the LW background, we take a similar approach to the one of the background produced by stars (Schauer et al. 2019) and use:

$$J_{\text{LW},21}^{\text{bg}}(z) = 10^{21} \frac{c}{4\pi} \int_z^{z_{\text{max}}} dz' \left| \frac{dt}{dz'} \right| \left(\frac{1+z}{1+z'} \right)^3 j_{\text{LW}}(z', z), \quad (17)$$

where dt/dz' denotes the cosmic time evolution with redshift, and j_{LW} gives the proper specific intensity defined as

$$j_{\text{LW}}(z', z) = L_{\text{LW}}(z', z) n(z), \quad (18)$$

where L_{LW} is the luminosity of the sources and n is their number density. The redshift z denotes the time when we estimate the background radiation, while z' covers the redshift range on which a different blackbody photon would be redshifted to the LW band at z , i.e. $\nu' = \nu_{\text{LW}}(1+z')/(1+z)$. The maximum redshift is estimated through the ‘screening approximation’, which assumes that the LW photons can travel through the intergalactic medium until they get absorbed by a Lyman line:

$$\frac{1+z_{\text{max}}}{1+z} = \frac{\nu_{\text{max}}}{\nu} = f. \quad (19)$$

Based on Visbal et al. (2014b), we assume $f \sim 1.04$.

Analysis of the LW background from stars in cosmological simulations provides an estimate of $J_{\text{LW},21}^{\text{bg}} \sim 3.6$ (Incataciato et al. 2023). We compare this with the case of a population of monochromatic PBHs. The proper specific intensity becomes:

$$\begin{aligned} j_{\text{LW}}(z) &= L_{\text{LW}}(z', z) n_{\text{PBH}}(z) \\ &= \frac{L_{\text{LW}}}{M_{\text{BH}}} M_{\text{BH}} n_{\text{PBH}}(z) \\ &= \frac{L_{\text{LW}}}{M_{\text{BH}}} f_{\text{PBH}} \rho_{\text{DM}}(z) \\ &= \frac{L_{\text{LW}}}{M_{\text{BH}}} f_{\text{PBH}} \Omega_m(z) \rho_{\text{crit}}(z) \\ &= \frac{4\pi^2 R_{\text{S}}^2 B_{\text{LW}}(z', z)}{M_{\text{BH}}} f_{\text{PBH}} \Omega_{m,0} (1+z)^3 \frac{3H_0^2}{8\pi G}, \end{aligned} \quad (20)$$

with

$$B_{\text{LW}}(z', z) = B_{\text{LW}} \left(\nu_{\text{LW}} \frac{1+z'}{1+z} \right), \quad (21)$$

and where we have connected the number density of PBHs to that of DM, and used the cosmological quantities defined in Appendix 9.1. Replacing $|dt/dz|$ with $1/(1+z)H(z)$ and substituting the expression for the proper specific intensity from eq. (20) into eq. (17) yields:

$$J_{\text{LW},21}^{\text{bg}} = 10^{21} \frac{c}{4\pi} \frac{4\pi^2 R_{\text{S}}^2}{M_{\text{BH}}} f_{\text{PBH}} \Omega_{m,0} \frac{3H_0^2}{8\pi G} \int_z^{z_{\text{max}}} dz' \left(\frac{1+z}{1+z'} \right)^3 \frac{B_{\text{LW}}(z', z)(1+z')^3}{(1+z')H(z')}, \quad (22)$$

which simplifies to

$$J_{\text{LW},21}^{\text{bg}} = 10^{21} \frac{cR_S^2}{M_{\text{BH}}} f_{\text{PBH}} \Omega_{m,0} \frac{3H_0^2}{8G} (1+z)^3 \int_z^{z_{\text{max}}} dz' \frac{B_{\text{LW}}(z', z)}{(1+z')H(z')}.$$
 (23)

For a quick estimate of its value, we observe that

$$\int_z^{z_{\text{max}}} dz' \frac{B_{\text{LW}}(z', z)}{(1+z')H(z')} \sim \frac{B_{\text{LW}}(\nu_{\text{LW}})}{(1+z)H(z)} \Delta z,$$
 (24)

where, as a reminder, we set ν_{LW} to the photons with energy in the middle of the LW band ($E_{\text{LW}} = 12.5$ eV) and have

$$\Delta z = z_{\text{max}} - z = (1+z_{\text{max}}) - (1+z) = (f-1)(1+z).$$
 (25)

Finally, this leads to

$$J_{\text{LW},21}^{\text{bg}} \sim 10^{21} \frac{cR_S^2 B_{\text{LW}}}{M_{\text{BH}}} f_{\text{PBH}} \Omega_{m,0} \frac{3H_0^2}{8G} (1+z)^3 \frac{(f-1)}{H(z)}.$$
 (26)

For $z = 10$ and $M_{\text{PBH}} = 4 \cdot 10^{-13} - 7.5 \cdot 10^{-12} M_{\odot}$, this results in $J_{\text{LW},21}^{\text{bg}} \sim 10^{-26} - 10^{-20}$, which is extremely small, and much smaller than the stellar contribution. Note that this more optimistic scenario is equivalent to assuming a flat spectrum in the LW band, and gives an upper limit. Therefore, the LW background radiation from PBHs does not play any role in blocking H₂ formation.

5. DISCUSSION

This section discusses the simplifying assumptions made in this paper, and assesses their influence on the results.

5.1. What happens with the production of other particles from HR?

In this paper, we have assumed that HR from PBHs consists only of massless particles – specifically, photons. In reality, HR can produce a variety of massless and massive particles (Page 1976; Frolov & Novikov 1998). These will be important for both the radiation signature of the black hole and its evolution. We comment on these impacts in order below, but first provide a simple estimate of when these effects are important.

As mentioned in Section 2, the temperature of HR is inversely proportional to the mass of a BH. As a result, as the BH shrinks it becomes more energetic and could have enough energy to emit massive particles. Ignoring neutrinos and taking the electron as the smallest nonzero-rest-mass particle, massless particles will dominate HR when:

$$k_B T \lesssim m_e c^2 \Rightarrow M_{\text{BH}} \gtrsim \frac{\hbar c}{8\pi G m_e} \Rightarrow M_{\text{BH}} \gtrsim 6.5 \times 10^{-17} M_{\odot} \sim 1.3 \times 10^{17} \text{ g}.$$
 (27)

When the BH masses are above this threshold, as is the case for the PBHs of interest in this work (see Section 4), considering only the primary spectra is a valid approximation. This regime is denoted by the region where $m_{\text{HR}} \rightarrow 0$ in Figure 4.

When the BH masses are below this threshold, massive particles start being produced⁶. These particles are not the final end products for an energetic BH since they can decay further (Arbey & Auffinger 2019; Lu et al. 2024). A percentage of these secondary particles would lead to the emission of additional photons – a ‘secondary spectrum’.

The effects of this extra emission are two-fold:

1. It will increase the emitted flux for a given BH. For the scenario investigated in this paper, the secondary spectra would strengthen the impact of HR by PBHs (see, for example, Figures 4 and 3 in Arbey & Auffinger (2021) and Auffinger (2023) respectively). In principle, focusing only on the primary spectra makes our analysis a conservative approach. However, the impact is negligible here since the mass regime of importance to our analysis (based on the constraints in Section 4) is greater than the mass threshold where the secondary spectra become significant.
2. It will lead to an increased rate of mass loss for a BH, expediting its evaporation (Mosbech & Picker 2022).

The mass evolution in this case is given by (Mosbech & Picker 2022):

⁶ This is a conservative threshold, since electrons and positrons would be ultra-relativistic at the range $m_e c^2 \ll k_B T \ll m_{\mu} c^2$, where m_{μ} is the mass of the muon. Taking this inequality into account by checking $k_B T \lesssim m_{\mu} c^2$, Page (1976) estimates that the massless particles approximation will break down for masses $M_{\text{BH}} \lesssim 10^{14}$ g.

$$M(t) = \left(M_i^3 - 3\alpha_{\text{eff}} \frac{\hbar c^4}{G^2} t \right)^{1/3}, \quad (28)$$

where $\alpha_{\text{eff}} = f(M)$ is a function of mass for $M_i \lesssim 10^{18}$ g, or a constant for $M_i \gtrsim 10^{18}$ g. For the ‘standard’ case we consider in this paper, $\alpha_{\text{eff}} = 1/15360\pi$. Although this would affect our determination of the evaporation time of a PBH, in the redshift and mass ranges we are considering, the PBHs are significantly far from evaporation and their evolution is effectively negligible (Figure 5). Therefore, this will not significantly affect our results.

5.2. Where are the ‘Greybody factors’?

In the original calculation of Hawking radiation (Hawking 1974; Traschen 2000) the number of emitted particles is

$$N_\nu = \Gamma_\nu \frac{1}{e^{h\nu/k_B T} - 1}, \quad (29)$$

where the Γ_ν term signifies the ‘greybody’ factor that modifies the spectrum from a perfect blackbody. It acts as the absorption coefficient for scattering of a scalar field off the gravitational field of a BH (Traschen 2000; Carroll 2019). In the short-wavelength/high-frequency limit where a photon has enough energy to surpass the effective potential due to the spacetime of the BH, this backscattering effect is small and can be ignored. To provide a quick estimate of where this limit occurs, we compare the wavelengths of the photons produced by HR with the Schwarzschild radius of the BH.

For the ‘greybody’ factors to *not* play an important role, the wavelength must be smaller than the Schwarzschild radius:

$$\lambda \lesssim R_S = \frac{2GM}{c^2} \Rightarrow M \gtrsim \frac{hc^3}{2GE} \quad \text{or} \quad \nu \gtrsim \frac{c^3}{2GE}, \quad (30)$$

where $E = h\nu$ is the energy of the radiated photon, and $c = \lambda\nu$ is the speed of light. Setting $E = E_{\text{LW}} \sim 12.5$ eV for the LW energy band provides the black hole mass threshold above which the ‘greybody’ factors can be ignored:

$$M_{\text{BH}} \gtrsim 3.35 \times 10^{-11} M_\odot \sim 6.68 \times 10^{22} \text{ g}. \quad (31)$$

The regime where ‘greybody’ factors may be ignored is denoted by the region where $\Gamma_{\text{greybody}} \rightarrow 1$ in Figure 4. The mass range of the PBHs of interest in this work (see Section 4), however, lie in this regime where $\Gamma \neq 1$. As such, we do need to take ‘greybody’ factors into account. In principle, codes calculating Hawking radiation deal with ‘greybody’ factors in a systematic way by also monitoring all of the particles that are produced (see Section 5.1). For simplicity, we instead multiply the spectrum by a constant ‘greybody’ factor, $f_\Gamma = 0.24$, based on values in Section IV and Table I of Page (1976). This constant factor corresponds to the ratio of photon power calculated numerically with the inclusion of the necessary ‘greybody’ factors to the photon power in the high frequency/energy limit.

5.3. Comparison to previous works

As shown in Section 4.4, none of the scenarios considered in this work contributed enough radiation to reach the critical LW threshold. This may seem in conflict with the recent results of Lu et al. (2024) where, under certain circumstances, PBHs were able to provide sufficient HR intensity to allow for direct collapse of the cloud. However, in reality, our work is complementary and consistent with their conclusions in the following ways:

- One main difference is that we are not considering evaporating BHs ($M_{\text{BH}} \sim 10^{14}$ g). The final ‘explosions’ of evaporating black holes produce high-energy radiation with an enhanced intensity due to the presence of significant secondary spectra. This explains the apparent disagreement with our work, which deals only with primary spectra and with masses of PBHs a few orders of magnitude bigger (and hence less energetic). Note that both mass ranges are viable; however, for our mass range, observational constraints allow $f_{\text{PBH}} = 1$, while for smaller PBHs ($M_{\text{BH}} \lesssim 10^{14}$ g) there are severe constraints leading to $f_{\text{PBH}} < 10^{-10}$ for the global fraction of PBHs.
- In our case, we are considering the intensity of HR from PBHs compared to the critical LW radiation required for the dissociation of H_2 , and other species connected to H_2 formation. The lack of these molecules lead to a reduced cooling rate, and hence the accumulation of bigger gas mass. This process is similar, but conceptually different from Lu et al. (2024) who consider the direct deposit of energy in the gas cloud.
- Lu et al. (2024) finds that significant PBH clustering is necessary inside the halos – about 7 orders of magnitude bigger than the external density, i.e. $f_{\text{PBH,in}} \sim 10^7 f_{\text{PBH,out}}$ – in order for collapse to a DCBH to occur. Although the models that we investigate do not produce radiation with sufficient intensity to surpass the CRI, the fact that

the isothermal distribution of PBHs gets closer to reaching the required CRI than does the uniform distribution of PBHs highlights – at least qualitatively – the importance of PBH density/clustering. Further analysis is required to determine if there are any extreme spatial distributions of PBHs within our mass range that could enable the collapse of a DCBH.

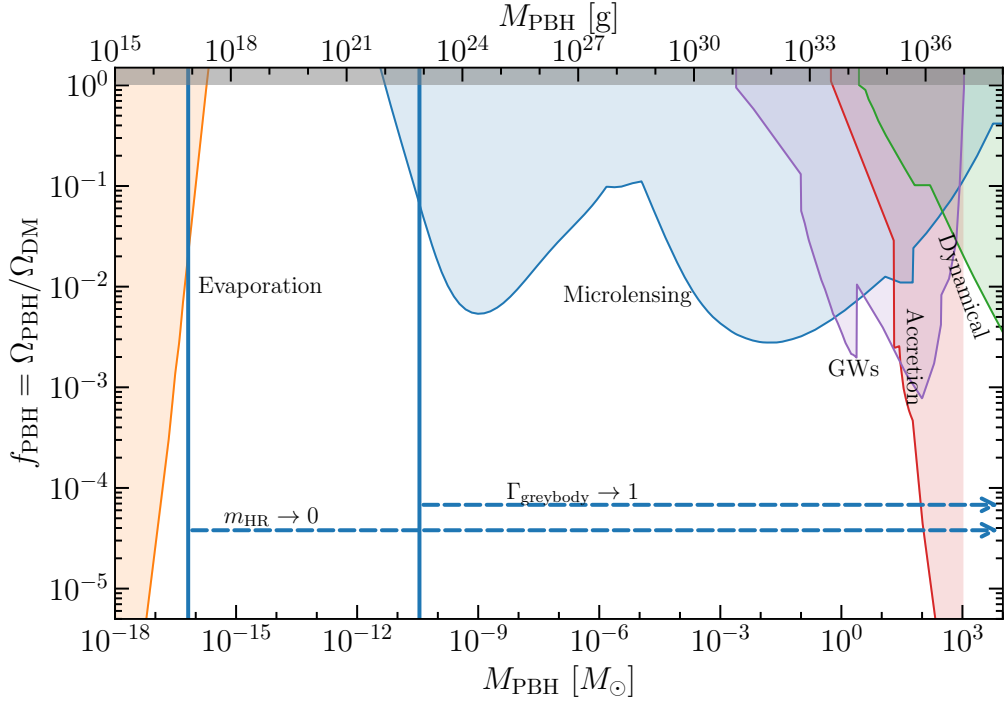


FIG. 4.— Similar to Figure 1, but now the dashed lines show mass ranges (specified by the arrows) where various assumptions are valid. $m_{\text{HR}} \rightarrow 0$ indicates the region where it is valid to only consider the primary HR spectra. The PBH mass range considered for this work *does* fall within this region of parameter space, and as such, we safely adhere to this assumption. $\Gamma_{\text{greybody}} \rightarrow 1$ indicates the region where it is valid to ignore greybody factors when calculating the HR spectrum. The PBH mass range considered for this work *does not* fall within this region of parameter space, and as such, we do account for a greybody factor. The y-axis values chosen for these are arbitrary and for visualization purposes only. For more details on these limits, see Sections 5.1 and 5.2.

6. CONCLUSIONS

The formation of supermassive black holes at the center of distant galaxies is an open question. Direct collapse black holes offer a solution. However, they require specific conditions in a primordial gas cloud in order to be formed – namely, the gas must remain warm enough, through a reduced cooling rate, and hence avoid fast and significant fragmentation to smaller clumps. In this work, we considered Hawking radiation from non-evaporating primordial black holes as the mechanism to destroy H_2 and related coolant species.

We used a simplified model of photon emission due to Hawking radiation from Schwarzschild black holes and calculated their specific intensity in the Lyman-Werner band, which plays a critical role in this scenario. We used physical constraints based on the evaporation timescale, X-ray emission, and temperature of primordial black holes to estimate a range of masses that is feasible for this scenario: $M_{\text{PBH}} \in (4 \cdot 10^{-13}, 7.5 \cdot 10^{-12}) M_{\odot}$. Interestingly, all values for the fraction of dark matter contained in primordial black holes are still allowed by observational constraints for this range of PBH masses. For PBHs within this mass range, we evaluated whether different spatial distributions of PBHs in or near a primordial gas cloud could produce the critical radiation intensity needed for the formation of a massive, atomic-cooling cloud, enabling it to directly collapse into a heavy seed for the early-Universe SMBHs that have been observed.

We conclude that non-evaporating PBHs cannot provide the radiation needed to facilitate the formation of massive black hole seeds since their radiation intensity is many orders of magnitude smaller than the expected critical value $J_{\text{crit}} \sim 5 - 1400$. Nevertheless, we exclude a range of masses of PBHs that could potentially have acted as ‘LW sources’. Additionally, we qualitatively confirm the importance of significant clustering of PBHs, recently proposed in the literature, when considering the effects of Hawking radiation from PBHs in enabling the formation of massive, atomic-cooling clouds.

7. ACKNOWLEDGMENTS

We would like to thank the referee for the very useful feedback that improved the clarity and quality of our paper. We also wish to thank the authors of Lu et al. (2024) for useful clarifications and feedback on our work. Additionally, we thank Boyan Liu for helpful comments on the PBH distributions and the analysis of LW radiation in Liu et al. (2022), Sadegh Khochfar for bringing to our attention the X-ray constraints and providing helpful comments and references, and Charalampos Tzerefos for comments and useful references on PBHs.

8. DATA AVAILABILITY

We make our code public in `DCBHs_HR_PBHs`.

9. APPENDIX

9.1. *Estimating halos sizes and masses*

We assume a simple model for halo formation, where the mass of the collapsing DM halo is given by Cimatti et al. (2020):

$$M_{\text{vir}} = \frac{4\pi}{3} \Delta_c \rho_{\text{crit}} r_{\text{vir}}^3, \quad (32)$$

where ρ_{crit} is the critical density to make the Universe flat:

$$\rho_{\text{crit}} = \frac{3H(z)^2}{8\pi G}, \quad (33)$$

with $H(z)^2 = H_0^2[\Omega_m(1+z)^3 + 1 - \Omega_m]$. The $\Delta_c = \rho_{\text{vir}}/\rho_{\text{crit}}$ depicts the overdensity of the halo and depends on cosmology and redshift. Using the fit provided by Bryan & Norman (1998) we have:

$$\Delta_c(z) = 18\pi^2 + 82y - 39y^2, \quad (34)$$

with $y = \Omega_m(z) - 1$ and $\Omega_m(z)$:

$$\Omega_m(z) = \frac{\Omega_{m,0}(1+z)^3}{\Omega_{m,0}(1+z)^3 + 1 - \Omega_m}. \quad (35)$$

Solving for the virial radius, yields:

$$r_{\text{vir}} = \left(\frac{2GM_{\text{vir}}}{\Delta_c(z)H(z)^2} \right)^{1/3}. \quad (36)$$

For a given redshift and a fixed halo mass, we use eq. (36) to get an estimate of the halo size.

Finally, the average density of the halo is given by $\rho_{\text{vir}} = \Delta_c \rho_{\text{crit}}$.

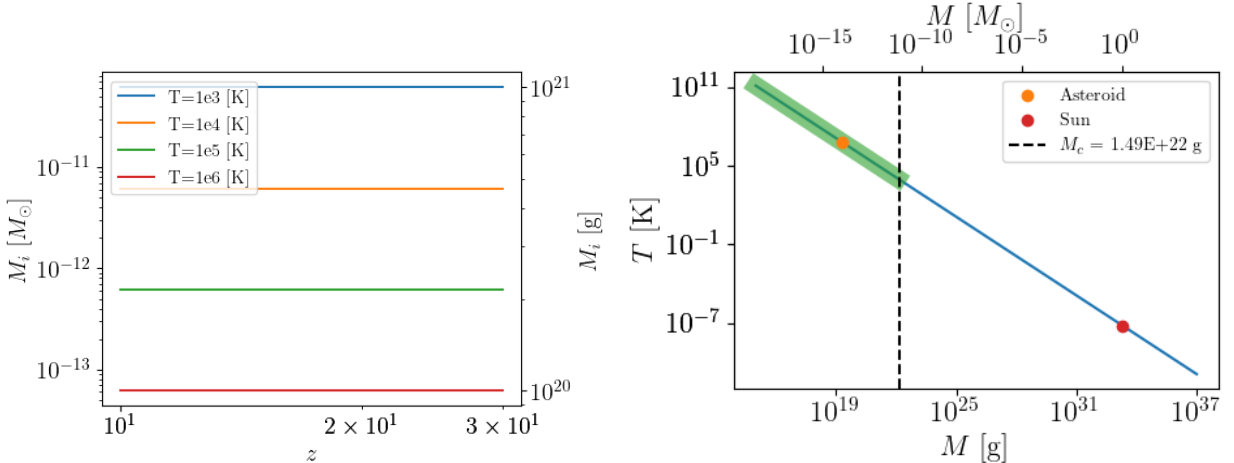


FIG. 5.— (a) PBHs evolution with redshift for specific temperatures of interest: Initial PBH masses for given blackbody temperatures in the redshift range of interest. In practice, the HR emitted from these BHs does not affect their mass evolution. (b) Mass range with effective blackbody HR temperatures above the critical value ($T_{\text{crit}} = 8000$): Relationship between Hawking temperature and BH mass. Data points show the Hawking temperature of some characteristic PBH masses. The green shaded region corresponds to effective blackbody temperatures above the critical temperature required to prevent the cloud from fragmenting. The dashed line quantifies the largest possible mass allowed by this constraint.

9.2. PBH evolution with redshift

Following the discussion of Section 2, we show the evolution of BH masses due to HR in the redshift range of interest ($10 \leq z \leq 30$) for four temperatures around the critical temperature ($T_{\text{crit}} = 8000$ K).

Figure 5 plots the initial mass of a PBH that would have a specific HR temperature as a function of redshift (found by solving eq. 7). For each temperature, the initial PBH mass needed is effectively the same for the entire range of redshifts. BH masses can only change significantly close to their evaporation time: for a PBH that would emit at around T_{crit} in the above redshift range, the evaporation time is estimated at 10^{24} Gyr, much larger than the age of the Universe.

Finally, we also note that for the mass ranges considered, PBH accretion is expected to be negligible (Rice & Zhang 2017).

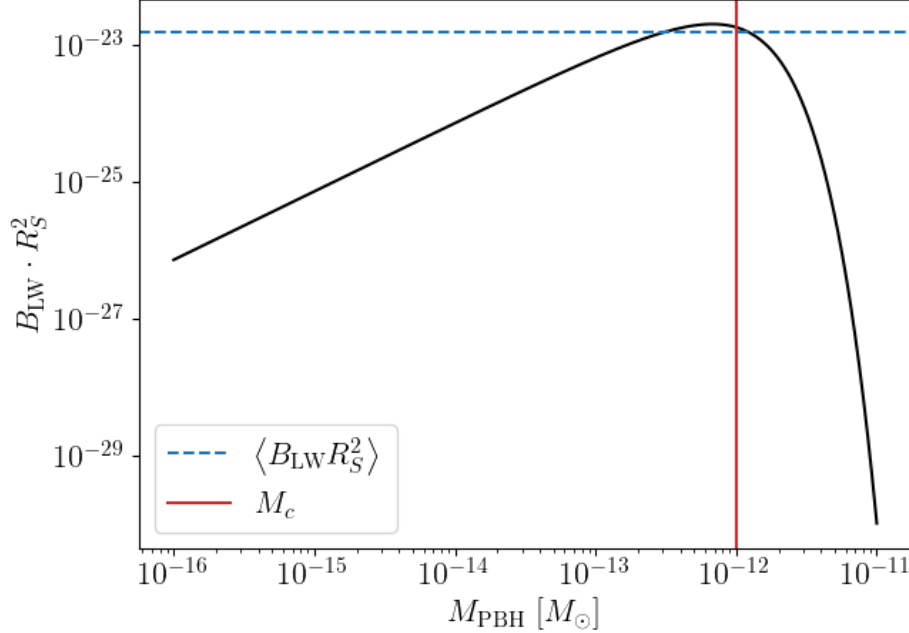


FIG. 6.— Change of $B_{\text{LW}} R_S^2$ with PBH mass. The dashed line shows the average value from the same range of masses for a specific PBH mass function.

9.3. PBH mass functions

At the time of formation, PBHs can have a range of masses that may follow one of several proposed model-dependent mass distributions (Chen & Hall 2024). Here, we show that a population of monochromatic PBHs – which is all that we consider in the main text – is sufficient to test the viability of the scenario at hand.

To demonstrate this, we consider the factor $B_{\text{LW}} R_S^2$ (the product of the specific intensity at the LW band with the squared Schwarzschild radius) since this factor plays the crucial role in determining specific intensity (see eq. 9). It is interesting to note that these two terms have an inverse behavior as a function of mass: the specific intensity gets bigger as the mass is reduced, while the Schwarzschild radius grows linearly with mass.

The mean value of this factor, $\langle B_{\text{LW}} R_S^2 \rangle$, over the relevant range of masses for some mass function $P(m)$ is given by:

$$\langle B_{\text{LW}} R_S^2 \rangle = \int_{M_{\text{min}}}^{M_{\text{max}}} B_{\text{LW}} R_S^2 P(m) dm. \quad (37)$$

We can quantify the importance of a given mass function by comparing this mean value to the value of $B_{\text{LW}} R_S^2$ calculated at each of the individual masses in the range. Figure 6 shows the $B_{\text{LW}} R_S^2$ product over a range of masses compared to the mean value of this factor for an example mass function. For demonstrative purposes, the mass function considered here is a log-normal mass function⁷

$$P_{\text{LN}}(m) = \frac{1}{\sigma m \sqrt{2\pi}} \exp \left(-\frac{\ln^2(m/M_c)}{2\sigma^2} \right), \quad (38)$$

⁷ Where $P(m)$ is normalized to unity: $\int_0^\infty P(m) dm = 1$.

where M_c denotes the median mass and σ the width of the mass distribution. Here, we chose a median mass near the peak of the $B_{\text{LW}} R_S^2$ product plotted in Figure 6: $M_c = 10^{-12} M_\odot$. Note that this also explains the dip in Figure 2(b). We also set $\sigma = 0.5$ so that the distribution is not very broad; however, the choice of σ does not affect the main conclusions.

Figure 6 demonstrates that a mass distribution, as expected from the properties of the mean, can outperform a number of individual masses but cannot surpass the maximum value of the $B_{\text{LW}} R_S^2$ distribution. Hence, choosing a PBH mass distribution can act as an optimistic choice, but will not alter the constraints of the best monochromatic PBH scenario.

REFERENCES

Agarwal B., 2019, in Latif M., Schleicher D., eds, , Formation of the First Black Holes. World Scientific Publishing, pp 115–124, doi:10.1142/9789813227958_0006

Agarwal B., Khochfar S., 2015, Monthly Notices of the Royal Astronomical Society, 446, 160

Agarwal B., Khochfar S., Johnson J. L., Neistein E., Dalla Vecchia C., Livio M., 2012, Monthly Notices of the Royal Astronomical Society, 425, 2854–2871

Agarwal B., Dalla Vecchia C., Johnson J. L., Khochfar S., Paardekooper J.-P., 2014, Monthly Notices of the Royal Astronomical Society, 443, 648–657

Agarwal B., Smith B., Glover S., Natarajan P., Khochfar S., 2016a, Monthly Notices of the Royal Astronomical Society, 459, 4209

Agarwal B., Johnson J. L., Zackrisson E., Labbe I., van den Bosch F. C., Natarajan P., Khochfar S., 2016b, Monthly Notices of the Royal Astronomical Society, 460, 4003–4010

Agarwal B., Cullen F., Khochfar S., Klessen R. S., Glover S. C. O., Johnson J., 2017, Monthly Notices of the Royal Astronomical Society: Letters, 468, L82–L86

Agarwal B., Cullen F., Khochfar S., Ceverino D., Klessen R. S., 2019, Monthly Notices of the Royal Astronomical Society, 488, 3268–3273

Arbey A., 2024, arXiv e-prints, p. arXiv:2405.08624

Arbey A., Auffinger J., 2019, European Physical Journal C, 79, 693

Arbey A., Auffinger J., 2021, European Physical Journal C, 81, 910

Auffinger J., 2023, Progress in Particle and Nuclear Physics, 131, 104040

Bañados E., et al., 2017, Nature, 553, 473–476

Bean R., Magueijo J., 2002, Physical Review D, 66, 063505

Becerra F., 2018, PhD thesis, Harvard University

Begelman M. C., 2010, Monthly Notices of the Royal Astronomical Society, 402, 673

Begelman M. C., Volonteri M., Rees M. J., 2006, Monthly Notices of the Royal Astronomical Society, 370, 289

Boekholt T. C. N., Schleicher D. R. G., Fellhauer M., Klessen R. S., Reinoso B., Stutz A. M., Haemmerlé L., 2018, Monthly Notices of the Royal Astronomical Society, 476, 366

Bromm V., Loeb A., 2003, The Astrophysical Journal, 596, 34

Bryan G. L., Norman M. L., 1998, The Astrophysical Journal, 495, 80

Byrnes C. T., Cole P. S., 2021, arXiv e-prints, p. arXiv:2112.05716

Carr B. J., 1975, Astrophysical Journal, 201, 1

Carr B. J., Hawking S. W., 1974, Monthly Notices of the Royal Astronomical Society, 168, 399

Carr B., Kühnel F., 2020, Annual Review of Nuclear and Particle Science, 70, 355

Carr B., Kohri K., Sendouda Y., Yokoyama J., 2021, Reports on Progress in Physics, 84, 116902

Carroll S. M., 2019, Spacetime and Geometry: An Introduction to General Relativity. Cambridge University Press, doi:10.1017/9781108770385

Chen Z.-C., Hall A., 2024, arXiv e-prints, p. arXiv:2402.03934

Chon S., Omukai K., 2024, arXiv e-prints, p. arXiv:2412.14900

Cimatti A., Fraternali F., Nipoti C., 2020, Introduction to Galaxy Formation and Evolution. Cambridge University Press

De Luca V., Desjacques V., Franciolini G., Malhotra A., Riotto A., 2019, Journal of Cosmology and Astroparticle Physics, 05, 018

Düchtig N., 2004, Physical Review D, 70, 064015

Escrivà A., Kuhnel F., Tada Y., 2022, arXiv e-prints, p. arXiv:2211.05767

Fan X., et al., 2003, The Astronomical Journal, 125, 1649

Frolov V. P., Novikov I. D., 1998, Black hole physics : basic concepts and new developments. Kluwer Academic

Green A. M., Kavanagh B. J., 2021, Journal of Physics G Nuclear Physics, 48, 043001

Haemmerlé L., Mayer L., Klessen R. S., Hosokawa T., Madau P., Bromm V., 2020, Space Science Reviews, 216, 48

Haiman Z., Rees M. J., Loeb A., 1997, The Astrophysical Journal, 476, 458

Haiman Z., Abel T., Rees M. J., 2000, The Astrophysical Journal, 534, 11

Hawking S., 1971, Monthly Notices of the Royal Astronomical Society, 152, 75

Hawking S., 1974, Nature, 248, 1

Hirano S., Hosokawa T., Yoshida N., Kuiper R., 2017, Science, 357, 1375

Hirano S., Machida M. N., Basu S., 2021, The Astrophysical Journal, 917, 34

Inayoshi K., Visbal E., Haiman Z., 2020, Annual Review of Astronomy and Astrophysics, 58, 27–97

Incatasciato A., Khochfar S., Oñorbe J., 2023, Monthly Notices of the Royal Astronomical Society, 522, 330

Johnson J. L., Dalla V. C., Khochfar S., 2012, Monthly Notices of the Royal Astronomical Society, 428, 1857–1872

Katz H., 2019, in Latif M., Schleicher D., eds, , Formation of the First Black Holes. World Scientific Publishing, pp 125–143, doi:10.1142/9789813227958_0007

Klessen R., 2019, in Latif M., Schleicher D., eds, , Formation of the First Black Holes. World Scientific Publishing, pp 67–97, doi:10.1142/9789813227958_0004

Klessen R. S., Glover S. C. O., 2023, Annual Review of Astronomy and Astrophysics, 61, 65

Koushiappas S. M., Bullock J. S., Dekel A., 2004, Monthly Notices of the Royal Astronomical Society, 354, 292

Kulkarni M., Visbal E., Bryan G. L., 2021, The Astrophysical Journal, 917, 40

Latif M. A., 2019, in Latif M., Schleicher D., eds, , Formation of the First Black Holes. World Scientific Publishing, pp 99–113, doi:10.1142/9789813227958_0005

Latif M. A., Ferrara A., 2016, Publications of the Astronomical Society of Australia, 33, e051

Latif M. A., Khochfar S., 2019, Monthly Notices of the Royal Astronomical Society, 490, 2706–2716

Latif M. A., Khochfar S., Schleicher D., Whalen D. J., 2021, Monthly Notices of the Royal Astronomical Society, 508, 1756–1767

Latif M. A., Whalen D. J., Khochfar S., Herrington N. P., Woods T. E., 2022a, Nature, 607, 48

Latif M. A., Whalen D., Khochfar S., 2022b, The Astrophysical Journal, 925, 28

Latif M. A., Schleicher D. R. G., Khochfar S., 2023, The Astrophysical Journal, 945, 137

Liu B., Bromm V., 2023, arXiv e-prints, p. arXiv:2312.04085

Liu B., Zhang S., Bromm V., 2022, Monthly Notices of the Royal Astronomical Society, 514, 2376

Liu B., Gurian J., Inayoshi K., Hirano S., Hosokawa T., Bromm V., Yoshida N., 2024, Monthly Notices of the Royal Astronomical Society, 534, 290

Lodato G., Natarajan P., 2006, Monthly Notices of the Royal Astronomical Society, 371, 1813

Loeb A., Furlanetto S. R., 2013, The First Galaxies in the Universe. Princeton University Press

Lovell C. C., Harrison I., Harikane Y., Tacchella S., Wilkins S. M., 2023, Monthly Notices of the Royal Astronomical Society, 518, 2511

Lu Y., Picker Z. S. C., Kusenko A., 2024, *Physical Review D*, 109, 123016

Mayer L., Bonoli S., 2019, *Reports on Progress in Physics*, 82, 016901

Merritt D., Milosavljević M., Favata M., Hughes S. A., Holz D. E., 2004, *The Astrophysical Journal*, 607, L9

Milosavljević M., Bromm V., Couch S. M., Oh S. P., 2009, *The Astrophysical Journal*, 698, 766

Mirbabayi M., Gruzinov A., Noreña J., 2020, *Journal of Cosmology and Astroparticle Physics*, 2020, 017

Mortlock D. J., et al., 2011, *Nature*, 474, 616

Mosbech M., Picker Z., 2022, *SciPost Physics*, 13, 100

Muñoz J. B., Qin Y., Mesinger A., Murray S. G., Greig B., Mason C., 2022, *Monthly Notices of the Royal Astronomical Society*, 511, 3657

O'Brennan H., Regan J. A., Power C., 2024, *arXiv e-prints*, p. arXiv:2408.15194

Oh S. P., Haiman Z., 2002, *The Astrophysical Journal*, 569, 558

Omukai K., 2001, *The Astrophysical Journal*, 546, 635

Omukai K., Palla F., 2001, *The Astrophysical Journal*, 561, L55

Page D. N., 1976, *Physical Review D*, 13, 198

Park J., Ricotti M., Sugimura K., 2021, *Monthly Notices of the Royal Astronomical Society*, 508, 6176

Rees M. J., 1984, *Annual review of astronomy and astrophysics*, 22, 471

Regan J., Volonteri M., 2024, *arXiv e-prints*, p. arXiv:2405.17975

Regan J. A., Wise J. H., O'Shea B. W., Norman M. L., 2020, *Monthly Notices of the Royal Astronomical Society*, 492, 3021

Reinoso B., Klessen R. S., Schleicher D., Glover S. C. O., Solar P., 2023, *Monthly Notices of the Royal Astronomical Society*, 521, 3553

Rice J. R., Zhang B., 2017, *Journal of High Energy Astrophysics*, 13, 22

Ricotti M., 2016, *Monthly Notices of the Royal Astronomical Society*, 462, 601

Schauer A. T. P., Liu B., Bromm V., 2019, *The Astrophysical Journal Letters*, 877, L5

Schauer A. T. P., Glover S. C. O., Klessen R. S., Clark P., 2021, *Monthly Notices of the Royal Astronomical Society*, 507, 1775

Schleicher D. R. G., Galli D., Glover S. C. O., Banerjee R., Palla F., Schneider R., Klessen R. S., 2009, *The Astrophysical Journal*, 703, 1096

Shang C., Bryan G. L., Haiman Z., 2010, *Monthly Notices of the Royal Astronomical Society*, 402, 1249

Smith A., Bromm V., 2019, *Contemporary Physics*, 60, 111

Sugimura K., Omukai K., Inoue A. K., 2014, *Monthly Notices of the Royal Astronomical Society*, 445, 544

Traschen J., 2000, in Bytsenko A. A., Williams F. L., eds, *Mathematical Methods in Physics*, p. 180 (arXiv:gr-qc/0010055), doi:10.48550/arXiv.gr-qc/0010055

Visbal E., Haiman Z., Terrazas B., Bryan G. L., Barkana R., 2014a, *Monthly Notices of the Royal Astronomical Society*, 445, 107

Visbal E., Haiman Z., Bryan G. L., 2014b, *Monthly Notices of the Royal Astronomical Society*, 445, 1056

Volonteri M., 2010, *The Astronomy and Astrophysics Review*, 18, 279

Volonteri M., Habouzit M., Colpi M., 2021, *Nature Reviews Physics*, 3, 732

Wise J. H., Regan J. A., O'Shea B. W., Norman M. L., Downes T. P., Xu H., 2019, *Nature*, 566, 85

Wolcott-Green J., Haiman Z., Bryan G. L., 2017, *Monthly Notices of the Royal Astronomical Society*, 469, 3329

Woods T. E., Heger A., Whalen D. J., Haemmerlé L., Klessen R. S., 2017, *The Astrophysical Journal Letters*, 842, L6

Workman R. L., et al., 2022, *Progress of Theoretical and Experimental Physics*, 2022, 083C01

Wu X.-B., et al., 2015, *Nature*, 518, 512

Yajima H., Khochfar S., 2016, *Monthly Notices of the Royal Astronomical Society*, 457, 2423–2432

Yajima H., Nagamine K., Zhu Q., Khochfar S., Vecchia C. D., 2017, *The Astrophysical Journal*, 846, 30